Biotech SI

https://doi.org/10.17113/ftb.63.02.25.8873 original scientific paper

Development and Application of a Novel 'Green' Antibacterial Black Garlic (*Allium sativum*)-Based Nanogel in Epidermal Wound-Healing

Running title: A 'Green' Antibacterial Black Garlic-Based Nanogel in Epidermal Wound-Healing

Mariah Sadaf[1], Anamika Das[1,2], Satadal Das[3], Subhankar Saha[4], Ketousetuo Kuotsu[4] and Paramita Bhattacharjee[1]*

[1]Department of Food Technology and Biochemical Engineering, Faculty of Engineering and Technology, Jadavpur University, 700032 Kolkata , India
[2]School of Bio-Science and Engineering, Faculty of Interdisciplinary Science and Technology, Jadavpur University, 700032 Kolkata, India
[3]Department of Microbiology, Peerless Hospital & B. K. Roy Research Centre, 70009 Kolkata 4, India
[4]Department of Pharmaceutical Technology, Faculty of Engineering and Technology, Jadavpur University, 700032 Kolkata, India

Received: 16 September 2024
Accepted: 27 May 2025

SUMMARY

Research background. Black garlic has been reportedly known to have several health promoting properties compared to fresh, raw garlic. Besides, it is reportedly known that the enzyme alliinase, which converts alliin to allicin is deactivated at a moderately high temperature and therefore strips the typical pungent odor of fresh garlic during fermentation and renders black garlic devoid of the "garlic-like smell". The alliin-rich extract obtained from black garlic powder has not been reported for its antimicrobial activity till date. The objectives of this study were: to explore the

*Corresponding author:
E-mail: paramita.bhattacharjee@jadavpuruniversity.in

antibacterial/antifungal activity of alliin-rich black garlic extract against *Staphylococcus aureus*, *Escherichia coli* and *Candida albicans*, and furthermore, based on the efficacy of the extract, formulate a topical drug using non-toxic, green ingredients in the form of a nanogel with promising wound-healing property and safe for human use.

Experimental approach. Authenticated fresh garlic (*Allium sativum*) cloves were first fermented to yield black garlic. Post fermentation, the brownish-black garlic cloves were peeled and ground into powder followed by Soxhlet extraction to obtain an alliin-rich extract. For the second objective, nanogels were formulated using the alliin-rich extract and were subjected to an *in vitro* release kinetics study. The antibacterial potency of the nanogels was also evaluated against *Staphylococcus aureus* (ATCC 29213) and *Escherichia coli* (ATCC 25922 and MDR), following which a skin irritation study was conducted on New Zealand albino rabbits.

Results and conclusions. Soxhlet extraction of pulverized black garlic cloves using distilled water yielded an alliin-rich extract (6.4 mg/100 g garlic), which also contained additional bioactive organosulfur compounds with no reported toxicity. The antimicrobial potency (in terms of its MIC value) of the extract was evaluated against potent skin pathogens and was found to be ~15 μg/mL. The nanogels formulated with the alliin-rich extract exhibited shear-thinning rheology and demonstrated admirable sensory properties when tested by a human panel. The *in vitro* release kinetics study revealed that there was a burst release of alliin (75 % of its content) from either gel within 5 min. Following skin irritation test performed in New Zealand white Albino male rabbits, no clinical signs of toxicity/mortality, redness or swelling were observed in the animals. Thereafter, the nanogels when applied individually on the epidermal wounds, prevented external infection and accelerated wound healing from day 2 onwards, achieving complete healing by day 7. Moreover, the gel with 4 % extract did not leave a scar on the wounded area after complete healing on day 7, establishing the same to be a promising topical antibacterial nanogel with accelerated epidermal wound-healing property, *vis-à-vis* a commercial broad spectrum topical gel used as a positive control.

Novelty and scientific contribution. This study is the first to report on a newly developed ‘green’ nanogel containing antimicrobial bioactives, namely, organosulfur compounds (diallyl disulfide, diallyl trisulfide, methyl-allyl-disulfide, methyl-allyl-trisulfide). The nanogel demonstrated promising epidermal wound-healing properties and thus holds promise in clinical applications against common and potent human skin pathogens.

Keywords: black garlic; alliin-rich extract; skin pathogens; epidermal wound-healing; antibacterial topical nanogel

INTRODUCTION

The underground bulb of fresh, raw garlic (*Allium sativum*) is consumed by human as a spice and as a medicine (*1,2*). It houses several bioactive components (*3*) which confer it strong antibacterial, antifungal, anti-inflammatory, and anti-allergic properties (*4,5*). The key bioactive compounds of raw garlic include organosulfur compounds, such as diallyl thiosulfonate (allicin), diallyl sulfide (DAS), diallyl disulfide (DADS), diallyl trisulfide (DATS), ajoene, s-allyl-L-cysteine, and alliin (*6*). Garlic cloves naturally store alliin and the enzyme alliinase separately. When garlic is crushed, alliinase converts alliin into allicin, which is responsible for the characteristic pungent odor of garlic (*7,8*).

Fresh garlic is fermented for 8–9 days under precisely controlled conditions of temperature (70–80 °C) and humidity (80–90 %) to produce black garlic (*9*), which is also known for its numerous health-promoting properties, including anti-oxidative, anti-allergic, anti-diabetic, anti-inflammatory, and cancer-preventive effects. It also has a longer shelf life compared to fresh, raw garlic (*6,10*). During fermentation, alliinase is deactivated in the temperature regime of 40–50 °C (*11*). This deactivation prevents the formation of allicin, thereby eliminating the typical pungent odor associated with fresh garlic (due to DADS), rendering black garlic free of the characteristic "garlic-like" smell (*12*).

While black garlic is known for its numerous health benefits, there is limited research on its antibacterial and antifungal properties. Recent research by Mouffok *et al*. (*13*) demonstrated the antibacterial potential of alliin-rich raw garlic extract against common human skin pathogens. However, there is a notable lack of research on the antimicrobial properties of alliin-rich black garlic extract. Furthermore, the potential correlations between the antibacterial and antifungal properties of black garlic extracts and their applications in topical skin treatments remain largely unexplored.

To prevent infection and promote rapid healing, antibacterial medications such as hydrogels, sponges, ointments, and nanogels are currently being widely used as effective drug delivery systems. Nanogels, in particular, offer distinct advantages over micro- and macro-scale hydrogels (*14*), including efficient drug loading, exceptional permeability across biological barriers, high water solubility, high thermal decomposition temperature, biocompatibility, and physical stability (*15,16*). To date, a solitary report exists on the formulation of a nanogel, based on allicin-rich raw garlic extract

(*17*), which is claimed to exhibit strong antifungal properties against *Candida albicans*. However, this nanogel is believed to retain the characteristic strong, pungent "garlic-like" odor, limiting its applicability for topical use. In contrast, an alliin-rich black garlic extract-based nanogel with similar antibacterial and antifungal potential would be more suitable for clinical use on the human skin, owing to its more acceptable sensory profile.

Carbopol® 940, a widely available polymeric carbomer known for its non-toxic and non-irritating properties (*18*), is commonly used in the development of stable nanogel systems that effectively encapsulate a range of bioactive compounds. In the present study, an alliin-rich Carbopol-based antibacterial nanogel has been developed to enhance epidermal wound healing.

Therefore, the specific objectives of the current investigation were to evaluate the antibacterial and antifungal activity of alliin-rich black garlic extract against *Staphylococcus aureus* (ATCC), *Escherichia coli* (ATCC and MDR), and *Candida albicans* (ATCC). Additionally, based on the efficacy of the extract, the study aims to formulate a topical drug in the form of a nanogel, utilizing non-toxic, green ingredients, with promising wound-healing property that is safe for human use.

MATERIALS AND METHODS

Materials

Authenticated fresh garlic (*Allium sativum*) was procured from Spencer's Retail store, Kolkata, India. Specialty chemicals such as alliin (>98 % HPLC grade) was procured from Sigma-Aldrich, Munich, Germany; L-α-phosphatidylcholine (lecithin soya 30 %) from HiMedia, Mumbai, India; silica gel 60 (F_{254}) coated Al plates from E-Merck, Mumbai, India; low density polyethylene (LDPE) Ziplock® pouches (dimensions 0.25 m×0.18 m) and Al foil from Prince Plastic Pvt. Ltd., Kolkata, India; and Mueller Hinton (MH) broth from HiMedia, Mumbai, India. American type culture collection(ATCC) strains of *Candida albicans*, *Staphylococcus aureus*, *Escherichia coli*, a multiple drug resistant (MDR) strain of *Escherichia coli* suspensions; and antibiotic discs of Augmentin were availed from Peerless Hospital, Kolkata, India. The grade of all chemicals and reagents utilized in this study was analytical reagent (AR) grade.

Fermentation of raw garlic

Authenticated fresh garlic was procured from Spencer's Retail store in Kolkata, India. The raw garlic samples were then stored in a rice cooker (Rize Excel 1.2 L, Kutchina, Kolkata, India) under warm mode (70–80 °C) with regulated high humidity (80–90 %) for 8–9 days to undergo controlled fermentation, in accordance with the method described by Lee *et al*. (*9*).

Preparation of black garlic powder

After fermentation, the brownish-black garlic cloves were peeled and ground into a fine powder using a mortar and pestle. The powder was then wrapped in Al foil and packaged in LDPE Ziplock® pouches. The pouches were subsequently stored in a desiccator until further analysis.

Soxhlet extraction of alliin from black garlic powder

The extraction of alliin from black garlic powder (10 g) was performed using a Soxhlet extraction apparatus with three different green solvent systems: water, a 1:1 ethanol-water mixture, and ethanol, in separate batches. Conventional Soxhlet extraction with *n*-hexane or petroleum benzene was not used, as alliin is water-soluble. Each extraction was conducted for 2 h with a 1:20 ratio of black garlic powder to solvent. The resulting extracts, obtained using water, ethanol-water, and ethanol as extracting solvents, were designated as BG_1, BG_2, and BG_3, respectively, and collectively referred to as BG_E.

Concentration of the black garlic extracts (BG_E)

The BG_E extracts (BG_1, BG_2 and BG_3) were concentrated using a rotary vacuum evaporator (R/160, Superfit Continental Private Ltd., Mumbai, India) at 5000 Pa and a water bath temperature of (45±2) °C for 25–30 min. The extracts were further concentrated to remove solvent residues, if any, by purging with nitrogen. The yields of the extracts were determined gravimetrically. Thereafter, the extracts were dissolved in distilled water and stored in amber-colored glass vials at -18 °C for subsequent analyses.

Quantification of alliin using high-performance thin layer chromatography (HPTLC)

The quantification of alliin content in the extracts (BG_E) was performed densitometrically with a Camag HPTLC unit (TLC scanner IV) at 450 nm using VisionCATS 3.0.20196.1 software (Muttenz, Switzerland) (*19*). The HPTLC analyses of BG_1, BG_2 and BG_3were conducted in accordance with the procedure outlined by Kanaki and Rajani (*20*) with slight modifications in the mobile phase composition. The extracts were applied in the form of 8 mm wide bands with 13.6 mm spacing between consecutive bands, using a Camag Linomat V (Camag, Switzerland) on Al TLC plates (200 mm×100 mm) coated with silica gel 60 (F_{254}). Chromatographic separation was achieved using *n*-butanol-acetic acid-water (6:2:2, by volume) as the mobile phase. The plate was then developed by spraying with a saturated ninhydrin reagent solution and heated at 100 °C for 5 min in a hot air oven. Visible brown color bands of varying intensities appeared on the developed plate.

Assessment of antimicrobial potencies of standard alliin and BG_E

Microbial culture suspensions of *Candida albicans* (ATCC 14053), *Staphylococcus aureus* (ATCC 29213) and *Escherichia coli* (ATCC 25922 and MDR) were used (0.5 McFarland standard) to evaluate the antimicrobial potencies of standard alliin and BG_E. The *in vitro* antimicrobial assays were conducted at Peerless Hospital, Kolkata, India, under the guidance of qualified microbiologists.

Determination of minimum inhibitory concentration (MIC) values of standard alliin and BG_E

The MIC values of standard alliin and BG_E were determined using the micro-broth dilution method (*21*) as outlined in a previous publication from our laboratory (*22*). BG_E was dissolved in distilled water to prepare a stock solution (1 mg/mL). Then, 100 µL of BG_E stock solution was added to each well of a sterile 96-well microtiter plate (0.5 McFarland was considered as the opacity standard), followed by inoculation with 10µL of microbial culture suspension. The plate was then incubated at 37 °C for 24 h. The turbidity of the mixture present in each well was assessed twice in terms of its absorbance measured at 620 nm: once immediately after addition of the microbial culture suspension to it, and again after 24 h of incubation, using a Multiskan™ FC Microplate Photometer (51,119,000,Thermo Scientific™, Massachusetts, USA). The respective MIC values were then evaluated from the graphical plot of the concentration of standard alliin and BG_E solution vs. turbidity. The extract with the lowest MIC value was selected for further analysis and coded as $BGE_{Best.}$

Compositional analysis and validation of presence of alliin in BGE_{Best} using electrospray ionization (ESI)-time-of-flight (TOF)-mass spectrometer (MS)

ESI-TOF-MS analysis of BGE_{Best} was carried out to validate the presence of alliin and to detect the presences of other key bioactive compounds of garlic, namely, organosulfur bioactive compounds such as DADS, DATS, methyl-allyl-disulfide and methyl-allyl-trisulfide. This was performed by a Xero-G2-Xs-QT, equipped with ADC-magnetron detector (Xero-G2-Xs-QT, WATERS, Milford, Massachusetts, USA), in accordance with the method described in our previous publication (*23*). The presence of alliin in BGE_{Best} was validated by comparing its mass spectrum with that of standard alliin and the presence of the organosulfur compounds were confirmed by comparing their mass spectra with those reported in the literature (*24)*.

Safety assessment of BGE_{Best}

Energy dispersive X-ray (EDX) of BGE_{Best}

Energy dispersive X-ray analysis of BGE_{Best} was performed using a scanning electron microscope (INSPECT F50, FEI Company, Hillsboro, OR, USA) to detect the presence of toxic heavy metals such as Pb, Hg, Ti, Ni, Si, As and Mo, if any. These metals could be either be inherent in raw garlic *per se*or potentially introduced during the processing stages (such as Soxhlet extraction).

Formulation of nanogels incorporating standard alliin and BGE_{Best}

Two sets of homopolymeric synthetic hydrogels, one using standard alliin and the other using BGE_{Best} were prepared following the methods described by Iizawa *et al*. (*25*) who had formulated poly (*N*-isopropylacrylamide) gel beads with physical cross-linking (*26*). Each hydrogel consisted of two phases, *i.e*. an organic and an aqueous phase. For the organic phase, a weighed amount of BGE_{Best} (based on the results of MIC value-*vide supra*) was dissolved in a mixture of dimethyl Sulfoxide (DMSO) (25.5 % *m*/*m*) as solvent and soya lecithin (0.5 % *m*/*m*) as an emulsifier, to increase the strength of the gel. This mixture was vortexed for 20 min followed by the addition of propylene glycol (74 % *m*/*m*) as moisturizer to improve drug permeation through animal/human skin surfaces. The resulting solution was then sonicated for 15 min at 25 °C using a bath sonicator (PCI Analytics, Mumbai, India).

For the aqueous phase, Carbopol® 940 (2% *m*/*m*), the gelling agent was stirred in distilled water (98 % *m*/*m*) using a magnetic stirrer(RCT B S022, IKA, New Jersey, USA) for a duration of 1 h at 1200 rpm at 80 °C. To ensure that the resultant gel was a nano-gel (*vide infra*), the gel was subjected to 2-stage homogenization using a homogenizer (Ultra-Turrax T-50 Basic Homogenizer, IKA, New Jersey, USA)- the first stage was carried out at 6000 rpm for 30 min, followed by a second stage at 8000 rpm for 45 min. During the second homogenization, the organic phase (~60 mL) was added incrementally (2 mL) to the aqueous phase every 5 min. No extract was added to the nanogel which served as the experimental control. Pure standard alliin (dissolved in DMSO) was added to the aqueous phase of the nanogel developed with standard alliin (standard gel).

Quantification of alliin in the standard gel and BGE_{Best} gel by HPTLC

To determine the content of alliin in the prepared hydrogels by HPTLC, 1 g of each hydrogel was dissolved in 2 mL distilled water. The solutions were vortexed followed by centrifugation (R-8C Remi Laboratory Centrifuge, Mumbai, India) for 5 min at 1500×*g* at 25 °C. A volume of 30 µL of the diluted supernatant solution(s) was used to measure the alliin content, according to the previously described procedure (*vide supra*).

Physicochemical characterization of the formulated gels

It was first necessary to evaluate whether the constituents of the gel were effectively incorporated into the matrix and the gels formed were indeed nanogels.

Fourier transform infrared spectroscopy (FT-IR) and attenuated total reflectance (ATR) analyses of the experimental control nanogel, BGE_{Best} nanogel and each gel constituent were carried out to confirm the successful incorporation of the gel components into the hydrogel matrix. FT-IR analysis of the individual constituents, *viz.* soya lecithin and Carpobol® 940 in powder forms was performed using KBr pellets and an FT-IR spectrometer (PerkinElmer, Massachusetts, US). ATR analysis of DMSO, propylene glycol, standard alliin solution, BGE_{Best}, experimental control hydrogel, and BGE_{Best} hydrogel in liquid form was conducted using a laser class I light source at a 45° angle of incidence. The FT-IR and ATR spectra were analysed using the wave numbers reported by Dyer (*27*) and it was found that all constituents had been successfully incorporated into the gel matrices (details elaborated later).

Field emission scanning electron microscope (FE-SEM) analysis of the hydrogels

The surface morphology and average particle size of the hydrogels were analysed using a FE-SEM (INSPECT F50, FEI Company, Oregon, USA) at an operating voltage of 5 kV. The gels (experimental control and BGE_{Best}) were dried and gold-coated using a Q150R ES Coater (Quorum Technologies Ltd., Kent, England). It was thereby confirmed that the hydrogels were truly nanogels (*vide infra*).

Specific gravity, pH, mass loss on drying, spreadability, phase separation and hydrophilic-lipophilic balance (HLB) value of nanogels (experimental control and BGE_{Best})

The physiochemical properties of the nanogels analysed were as follows: specific gravity using a pycnometer, pH using a digital pH meter (pc 510, Eutech Instruments, West Bengal, India); percentage mass loss on drying (at 105°C) using the method described by Buhse *et al*. (*28*). The spreadabilities of the nanogels were evaluated following the method described by Ghosh *et al*. (*29*) using the equation:

$$S=(m\cdot l)/t \qquad /1/$$

where S=spreadability of the nanogel, m=mass attached (66 g), l=length of glass slide (7.5 cm) and t=time.

The viscosities of the nanogels were determined using the Brookfield Digital Viscometer (LVDVE230, Brookfield Engineering Company, MA, USA), model LVDV-E with spindle no. 4 (S_{64}) at (25±1) °C. The fluid behaviour was described using the consistency index, which was determined by fitting the data into different model equations. The plot was constructed using logarithm of shear stress and shear strain and the consistency index was calculated.

The formulated nanogels were centrifuged at 2500×*g* (TC-4815D,Eltek, Mumbai, India) and phase separation studies were performed in a water bath (Techno-Lab and Instrumentations, India) at 37 and 55 °C, respectively, in accordance with the procedures elaborated by Widodo *et al*. (*30*). The HLB values for the nanogels [HLB = 20 (1-S/A), where, ‘S’ is saponification value and ‘A’ is acid value] were determined according to the procedure described in Fennema’s Food Chemistry (*31*).

Release profile study of BGE_{Best} nanogel

The release profile of alliin from the BGE_{Best} nanogel was investigated using the methodology described by Ghosh *et al*. (*29*). A mass of 0.5 g of BGE_{Best} nanogel was mixed with 50 mL of phosphate buffer saline (PBS) solution (0.1 M, pH=7.2). The mixture was continuously stirred for a duration of 2 h at 50 rpm (~34 °C) using a magnetic stirrer (RCT B S022, IKA, New Jersey, USA).3 mL aliquot was withdrawn at an interval of 5 min for a period of 2 h and was replaced with a similar amount of fresh PBS solution. The alliin content in the nanogel was determined using the HPTLC method described above.

Analyses of antibacterial potencies of standard alliin and BGE_{Best}-based nanogels

MH agar plates were prepared by dissolving 3.8 g of MH agar powder (HiMedia, Mumbai, India) in 100 mL of sterile (autoclaved) distilled water.

Kirby-Bauer disk diffusion susceptibility test

The zones of inhibition against uniform suspensions of *Staphylococcus aureus* (ATCC 29213) and *Escherichia coli* (ATCC 25922) and the MDR strain of *Escherichia coli* (0.5 McFarland standard) were evaluated using the Kirby-Bauer disk diffusion susceptibility test (*32*).

Animal study on skin irritancy and assessment of wound-healing property of BGE_{Best} nanogel on rabbits

The skin irritation test and assessment of wound-healing efficacy of BGE_{Best} nanogel were conducted at the Clinical Research Centre of Jadavpur University, in collaboration with professional experts in clinical pharmacology. For the tests, four healthy New Zealand white Albino male rabbits (R1, R2, R3, R4), aged 6-8 months, weighing 1.5–1.8 kg were procured from Reeta Ghosh Private Ltd., West Bengal, India. Prior to the experiments, the animals were placed in separate cages and allowed to get acquainted to the test environment (22 ºC, 60–70 % relative humidity (RH) with a 12 h cycle of light and darkness) for 7 days. Ad-labium food and drinking water were provided to all animals for the entire duration of the experiment (*29,33*).

For future safe use in humans, it was necessary to conduct the skin irritation test on the rabbits (R1, R2, R3, R4) according to the Organization for Economic Co-operation and Development (OECD) Test Guideline 404 (*34*). The skin irritation test was conducted in accordance with the Draize dermal irritation scoring system (*35*) and subsequent evaluation of the wound-healing property of the BGE_{Best} nanogel was performed in accordance with the methodology described in a previous publication of our laboratory (*22*).

Approximately 24 h prior to the skin irritation test, the fur on the dorsolateral trunk of each rabbit was removed carefully and a patch of 5 cm×5 cm area was created, on which a small quantity of BGE_{Best} nanogel was uniformly applied on the day of the experiment. To assess skin irritancy, the rabbits (R1, R2, R3, R4) were observed immediately following the application of BGE_{Best} nanogel and subsequently after 24, 48 and 72 h. All four animals were observed regularly for signs of allergic reactions, clinical toxicity, mortality or morbidity, until the completion of the experiment.

Full-thickness skin, including the panniculus carnosus layer was excised from a demarcated area to create an epidermal wound of approximately (7.5±2.5) mm² on each rabbit. The wound sites were gently cleansed using sterile cotton swabs. After cleansing, the following formulations were applied: a commercially available positive control gel to rabbit R1, an experimental control nanogel to R2, 2 % BGE_{Best} nanogel to R3, and 4 % BGE_{Best} nanogel to R4. These formulations were topically applied to the wound sites twice daily until complete epithelialization and wound closure occurred.

The physical parameters of wound healing, including wound closure, epithelialization time and scar characteristics were assessed throughout the study. Wound closure was monitored by tracing the raw wound margins onto transparent tracing paper at regular intervals from day 0 to the final day of the experiment. The wound area was calculated by counting the number of enclosed squares after transferring the traced outline of the retraced wound area on a 1 mm^2 graph paper. The degree of wound healing was calculated as percentage closure of the wound area from the original one using the following formula:

$$\text{Percentage closure} = [1-(A_d/A_0)]\cdot 100 \qquad /2/$$

where A_0 is the wound area on day zero and A_d is the wound area on corresponding days.

Storage stability studies of the BGE_{Best} nanogel

The storage stability of BGE_{Best} nanogel was investigated by assessing its alliin content during its storage at (4±1) °C for 12 months in the dark. Amount of alliin retained in the gel was determined by HPTLC analysis performed at an interval of 10 days. Half-life ($T_{1/2}$) of the BGE_{Best} nanogel was calculated by assessing its alliin content densitometrically. The ratio of alliin content on day 0 (TA_0) and on day *t* (TA_t) for the gel sample was estimated and the natural logarithm (ln) of TA_0/TA_t was plotted against storage time (*t*). The slope of the line (*k*) was used to obtain the half-life ($T_{1/2}$=ln 2/*k*) of alliin in the BGE_{Best} nanogel.

The storage stability of the BGE_{Best} nanogel was evaluated by assessing its microbiological properties, primarily antibacterial activity, and visual mold growth, as well as its sensory and physicochemical characteristics. Two sample sets were prepared: one set was stored at (23±2) ºC with 70–75 % relative humidity for 30 days (as previously described), while the other set was stored at (4±1) ºC in the dark for 12 months.

Sensory evaluation of the experimental control and BGE_{Best} nanogels

The sensory evaluation of the nanogels was carried outat three stages of application on the skin: ‘before rubbing and during pick up’, ‘during rubbing’ and ‘after-feel’ where in various parameters such as stiffness, grittiness, color, odor, homogeneity, stickiness, shine, absorbance, skin feel, and spreadability were evaluated (*36*). The evaluation was conducted by six semi-trained panellists comprising of university research scholars in the age group of 25–34 years (three males and three females) on day 1 and day 30 of storage. The subjects were found to be non-allergic to the ingredients of the nanogel formulations and had no skin diseases. They were acquainted with the various parameters of the sensory (cosmetic) properties of the nanogels. The evaluations were carried out in a well-illuminated-cum-ventilated room. Before application, the skin surface and fingers of the panellists were wiped with clean sterile cotton. The panellists applied the nanogels on the back of their hands using ten circular movements. The responses of the panellists were recorded by rating the nanogels on a five-point hedonic scale (ranging from -2 to 2; word anchors ranging “dislike very much” to “like very much”) according to the method described by Almeida *et al*. (*37*).

Statistical analyses

In this study, extraction, microbiological and physicochemical assays were conducted in triplicate and the results are presented as mean value±S.D. of three independent analyses of three independent batches of samples. Statistical analyses were performed using one-way analysis of variance (ANOVA). A value of $p \leq 0.05$ was used to verify the significance of all assays. All statistical analyses were conducted using IBM SPSS Statistics software v. 26 (*38*).

RESULTS AND DISCUSSION

Characteristics of black garlic powder and extract

Post fermentation of raw garlic, the white garlic cloves attained a brownish black colour and the characteristic garlic odor was diminished. From these fermented black garlic cloves, ~95.67 % of powder with average particle size diameter (d_p) ~55 μm was obtained.

A mass of 1.27–4.96 g of Soxhlet extracts of black garlic were obtained after vacuum concentration. The lowest yield of black garlic extract (1.27 g) was obtained when ethanol was used as the extraction solvent (BG_3), while the highest (4.96 g) yield was achieved using ethanol: water (1:1) as used as the solvent system (BG_2). Water as extraction solvent yielded 4.54 g extract (BG_1).

Alliin contents in BG_1 and BG_2

The alliin (R_f value=0.82) contents in BG_1 and BG_2 were found to be 1.8 and 1.322 mg/g, respectively (Fig. S1). However, alliin could not be quantified in BG_3 owing to its poor solubility in ethanol (*39*) which was used as an extraction agent (*vide supra*). BG_1 had the highest content of alliin ($p \leq 0.05$) as alliin is highly soluble in water (*40*).

Antimicrobial potencies of standard alliin and BG_E

MIC values of standard alliin were 10, 40, 70 and 75 μg/mL for *Candida albicans* (ATCC 14053), *Staphylococcus aureus* (ATCC 29213) and *Escherichia coli* (ATCC 25922 and MDR), respectively. On an average, the MIC value of BG_1 was 15 μg/mL against the above-mentioned bacterial strains [*Staphylococcus aureus* (ATCC 29213) and *Escherichia coli* (ATCC 25922 and

MDR)] and that of BG_2 was 25 μg/mL for the same. The MIC values of both BG_1 and BG_2 were much higher (>90 μg/mL) against the above-mentioned fungal strain *Candida albicans* (ATCC 14053). Based on these results, it can be inferred that although standard alliin demonstrates potent antimicrobial activity, the antibacterial properties of BG_E were stronger than its antifungal properties. Based on the results of the one-way ANOVA for the MIC values of standard alliin and BG_E (BG_1 and BG_2), it can be concluded that BG_1 exhibited a significantly lower MIC value ($p \leq 0.05$), indicating its superior ability to inhibit bacterial growth *vis-à-vis* BG_2. Considering higher antibacterial activity, BG_1 was designated as BGE_{Best} and used for formulation of the nanogel.

To the best of our knowledge, there is no available literature on alliin content in white and black garlic and none on antimicrobial potency of alliin-rich black garlic extract to allow comparison of our findings.

Composition and safety of BGE_{Best}

Based on the ESI-TOF-MS spectrum of the pure standard of alliin (Table 1), it was confirmed that the alliin content quantified by HPTLC in BGE_{Best} corresponds unequivocally to the target biomolecule, alliin. A similar ESI spectrum for alliin has been reported by Tran *et al*. (*41*).

From the *m*/*z* values ranging from 143 to 180 in the ESI-TOF-MS Spectra (Table 1) of BGE_{Best} (*24*), several additional organosulfur bioactive compounds such as di-allyl-disulfide, di-allyl-trisulfide, methyl-allyl-disulfide and methyl-allyl-trisulfide were tentatively identified. These organosulfur compounds present in black garlic extract are reportedly non-toxic (*6*), and possess antibacterial and antifungal properties (*4,5*).

The EDX spectra of BGE_{Best} (figure not shown) did not reveal peaks of heavy metals, thereby confirming the absence of heavy metal contaminants in the formulation. These findings affirm the extract to be non-toxic and therefore safe for the formulation of a topical antibacterial nanogel for potential human clinical application.

Physicochemical properties of the nanogels incorporated with standard alliin and BGE_{Best}

The standard alliin-based nanogel was odourless and clear in appearance; while the BGE_{Best} nanogel had a pale-yellow colour and translucent appearance with a slight garlic characteristic odor.

FT-IR and ATR spectra of Carbopol® 940, DMSO, propylene glycol, lecithin soy (30 %), standard alliin, BGE_{Best}, experimental control nanogel and BGE_{Best} nanogel

The transmission (*T*/%) peaks of the BGE_{Best} nanogel were similar to those of the standard alliin solution. The transmission peaks of nanogels matched those of the individual components in the formulation. FT-IR and ATR analyses confirmed that the Soxhlet extract (BG_1), which is rich in alliin, had been effectively incorporated into the nanogel matrix.

The functional groups and the absorbance bands prominently present in the FT-IR spectraof the analysed samples are presented in Table 2. The spectra showed the presence of O-H stretching (3628, 3348 cm^{-1}), C-H stretching (2853 cm^{-1}), C=C alkene stretching (1651 cm^{-1}), C-O-C stretching (1249, 1225 cm^{-1}) and C-F stretching (1044, 1016 cm^{-1}), which confirmed the presence of standard alliin in the BGE_{Best} nanogel, along with the other ingredients in the formulation.

Microstructure of the experimental control and BGE_{Best} nanogels

The FE-SEM analyses revealed that the experimental control and BGE_{Best} nanogels had a smooth spherical surface morphology. The average particle size was 286.06 and 217.77 nm for the experimental control and BGE_{Best} nanogels, respectively (Fig. 1), which aligns well with the dimensions of other reported nanogels, such as of kappa-carrageenan/chitosan (*42*). From the findings, it can be inferred that the average particle size of the formulated gel was in the nanometer range and thus the same can be classified as a nanogel.

Specific gravity, pH, mass loss on drying, spreadability, phase separation and HLB values of nanogels (experimental control and BGE_{Best})

The physicochemical analyses of the formulated topical nanogels are listed in Table 3. The pH values of 6.90 and 6.82 for the control and BGE_{Best} nanogels, respectively, were well within the range suitable for use as a topical medication compatible with the human skin (*43*). Similar pH values were reported by Wadile *et al*. (*44*) for their nanogel incorporated with itraconazole nanoparticles (pH=6.8); and by Ali *et al*. (*45*) who reported a pH of 6.87 for lidocaine wound-healing nanogel. The specific gravities of nanogels were 1.038 for the control and 1.021 for the BGE_{Best} nanogel, respectively, and the percentage weight loss on drying was 2.31% for the control and 1.5% for the BGE_{Best} nanogel (dry basis). The spreadability of nanogel, a crucial aspect which influences its viscosity and cosmetic

(sensory) acceptability (*46*), was found to be 15.92 g/(cm·s) for the control and 12.41 g/(cm·s) for the BGE_{Best} nanogel. A similar value for spreadability has been reported by Inamdar *et al*. (*47*) for nanogel loaded with β-sitosterol as its bioactive component.

The plot of log shear stress *vs*. log shear rate (Fig. S2) showed that the nanogels are non-Newtonian fluids. Model fitting revealed that viscosity data best fit the modified Casson equation:

$$\log \tau = \log \mu_{app} + n \log (\partial u / \partial y) \quad /3/$$

where τ is shear stress (dyne/cm); $\partial u / \partial y$ is shear rate (s^{-1}); μ_{app} is apparent viscosity (cP) and n is flow behavior index.

The flow index (n<1) using the above equation indicates that the nanogels exhibit pseudoplastic flow behavior. Eq. 3 shows that the apparent viscosity of the control nanogel is 18.92 cP and that of the BGE_{Best} nanogel is 23.03 cP. Since the nanogels are shear-thinning and have appreciable spreadability, they are advantageous for effortless topical application. A similar flow behavior was reported by Agarwal *et al*. (*48*) for a semi-herbal clindamycin phosphate aloe-vera nanogel. No phase separation on centrifugation at 37 and 55 °C indicated that the formulation was properly homogenized. HLB value for the experimental control nanogel was 17 and that for the BGE_{Best} nanogel was 18.6 indicating that the formulation was hydrophilic (*31*).

In vitro release profile of BGE_{Best} nanogel

The BGE_{Best} nanogel exhibited a 75 % burst release of alliin within 5 min, indicating a high release rate. This rapid release is advantageous for immediate drug delivery upon topical application, making it beneficial for wound-healing (*49*). Reports are scanty on *in vitro* release kinetics study of topical hydrogels/nanogels; however, a similar burst release of dexamethasone from PNIPAM-co-acrylic acid hydrogels in the submicron range has been observed by Gu and Burgess (*50*).

Antibacterial potencies of formulated nanogels

Kirby-Bauer disk diffusion susceptibility test

The standard alliin-based nanogel exhibited a zone of inhibition of 7 mm for *Staphylococcus aureus* (ATCC 29213), and that for BGE_{Best} nanogel was 10 mm. For *Escherichia coli* (ATCC 25922),

the zone of inhibition was 7 mm for the standard alliin-based nanogel, and 8 mm for the BGE_{Best} nanogel; and for MDR strain of *Escherichia coli,* it was 6 mm for the standard alliin-based nanogel, and 7 mm for the BGE_{Best} nanogel (Fig. S3). From one-way ANOVA of the diameters of the zones of inhibition of standard alliin-based nanogel and of the extract-based nanogels, it can be concluded that the BGE_{Best} nanogel had significantly ($p \leq 0.05$) greater antibacterial potency compared to the standard alliin-based nanogel, rendering the test nanogel as a potent therapeutic formulation for topical wound-healing.

Animal study on skin irritancy and wound-healing property on rabbits

Skin irritation test of BGE_{Best} nanogel on rabbits

The primary irritation index (PII) scores of the nanogel for erythema and edema were zero after 72 h, which implied that there were no indications of skin irritation at the test site during the period of study (Fig. S4). Following the application of the nanogel to the skin surface, the rabbits exhibited no clinical signs of toxicity or irritation. Therefore, it can be concluded that the BGE_{Best} nanogel is a safe, non-toxic formulation with no adverse irritant effects [PII (0/36=0)] when applied to rabbit skin. This suggests that the nanogel can safely be used topically to evaluate its efficacy in promoting epidermal wound-healing.

Wound-healing efficacy of BGE_{Best} nanogel

Fig. S5a and Fig. S5b represent the epidermal wound-healing experiment using BGE_{Best} nanogels (2 and 4 %) on R3 and R4, respectively (Table 4). Following topical application, tissue epithelialization surrounding the injuries (in R3 and R4) commenced on day 2. By the end of day 6, 67 and 77 % of wounds had healed in R3 and R4, respectively; which was found to be almost similar to the wound-healing efficacy of the positive control gel which achieved 86 % wound closure by day 6 in R1. In contrast, the control nanogel showed no signs of wound closure in R2, confirming that the experimental control nanogel alone did not contribute to wound healing, thereby validating the wound-healing properties of BGE_{Best} nanogel.

Results from the one-way ANOVA analysis of wound-healing areas, following the application of the positive control gel, experimental control nanogel, and 2 and 4 % BGE_{Best} nanogels in the

respective animal groups on a daily basis, indicated that the wound-healing efficacy of the 4 % BGE_{Best} nanogel (in R4 group) was significantly ($p \leq 0.05$) superior to that of the 2 % BGE_{Best} nanogel (in R3 group). The healing process in the R4 group was notably accelerated. Furthermore, the wound sites were effectively protected from any external infection by applying 2 % BGE_{Best} nanogel in R3 and 4 % BGE_{Best} nanogel in R4. By day seven, the wound in R4 healed had completely healed with no scarring, confirming that the 4 % BGE_{Best} nanogel is a promising topical antibacterial nanogel with enhanced wound-healing properties.

A study reported by Ahmed *et al*. (*51*) revealed similar findings of accelerated wound-healing in rabbits using a hydrogel formulated with the herb *Centella asiatica*. At the end of day 5 of treatment, wounds treated with the hydrogel showed complete wound closure with the formation of a thin epidermal layer; and by the end of day 9, all wounds were healed with a concomitant thickening of the epidermis layer. The wound reduction in rabbits treated with *Centella asiatica* hydrogel was approximately 40% higher compared to the untreated wounds in the control group of rabbits (*51*).

Stability of the BGE_{Best} nanogel

The half-life ($T_{1/2}$) of the BGE_{Best} nanogel was approximately 193 days, although the alliin content remained above its MIC until 120 days of storage. After this period, the alliin content gradually decreased to below the MIC value (<15 μg/mL). Therefore, it is recommended to store the BGE_{Best} nanogel at (4±1) °C and use it within 120 days to ensure optimal effectiveness.

Sensory attributes of the experimental control and BGE_{Best} nanogels

During sensory evaluation of the nanogels, the panel preferred the non-sticky consistency and shiny appearance of BGE_{Best} nanogel. Both the experimental control and BGE_{Best} nanogel were non-irritable, easily spreadable, moderately slimy, and very shiny with good to moderate absorption capacity (Fig. 2). The findings suggested that the panel validated the formulation as a topical nanogel with moisturizing property. Based on the radar plot analysis of the hedonic scores obtained using the 9-point hedonic scale, it is seen that BGE_{Best} nanogel had the highest score (9) for spreadability and absorption, *vis-à-vis* 8 and 6, respectively, for the control set of nanogel. Not only the BGE_{Best} nanogel was preferred over the control nanogel for its superior skin spreadability and absorption, other

cosmetic characteristics such as color, odor, homogeneity and textural features (stickiness and skin-feel) were more sensorially appealing for the same.

The shear-thinning characteristic of BGE_{Best} nanogel made it more spreadable, which led to good absorption and great primary and secondary skin feel, as is evident (Fig. 2) from their sensory scores (*52*). The nanogel could be spread evenly on the skin surface without being highly adhesive or tacky (*30*). The safety of the nanogel for future clinical studies was further validated by the skin irritation test in rabbits as has been discussed above. The present study has conclusively demonstrated the potential of black garlic extract based-nanogel for topical application.

Comparison of the newly formulated nanogel with reported gels having wound-healing properties

These attributes align well with pharmaceutical recommendations for effective topical delivery of active ingredients through the human skin, as has been reported by Kulawik-Pióro *et al*. (*53*), who investigated the quality of barrier creams [composed of International Nomenclature of Cosmetic Ingredients (INCI) ingredients namely, aqua, glycerine, sodium silicate, sodium palm kernelate, ceteareth-5, sodium tallowate, cera alba, paraffin, parfum *etc*. with similar attributes.

A commercially available and commonly prescribed gel used for wound-healing is Hydroheal AM gel, which is formulated with non-green, toxic ingredients (colloidal silver) and is known to cause argyria, a permanent bluish-grey skin discoloration, when applied to human skin for prolonged periods. It can also interfere with the absorption of drugs and lead to potential problems in kidney, liver, and the nervous system (*54*). Moreover, since colloidal silver is one of the main constituents in this gel, it cannot be used to heal open wounds because the silver oxidizes readily in atmospheric air and produces silver oxide that may cause greyish-black discoloration when applied to the skin (*55, 56*). Thus, to overcome this disadvantage, it is advisable that the commercial gel can only be used prior to the epidermal/dermal wound dressing and thereafter, the wound must be bandaged to prevent direct air contact.

On the contrary, the newly formulated BGE_{Best} nanogel contains a safe, toxicity-free organosulfur compound containing, alliin-rich black garlic extract and non-toxic, green ingredients which is completely safe for human application against common potent skin pathogens and for long-term usage to heal open epidermal wounds with promising efficacy.

CONCLUSIONS

This study is the first to describe the antibacterial activity of a safe, green nanogel loaded with toxicity-free alliin-rich black garlic extract. The resulting yellow tinted nanogel exhibited significant antibacterial activity against the common bacterial pathogens *S. aureus* and *E. coli*. The nanogel formulation produced homogeneous, spherical, lump-free particles in the nanometer range with a smooth surface morphology. With a pH range of 6.82 to 6.90, BG_1 outperformed BG_2 in terms of drug content and MIC value. The formulated nanogel can be used for topical application with ease owing to its excellent spreadability and viscosity. The spreadability value for BGE_{Best} nanogel along with its pseudoplastic behavior further supports its use for topical applications. FT-IR and ATR analyses confirmed the successful integration of alliin-rich BGE_{Best} into the nanogel matrix along with its other components. Skin irritation and epidermal wound-healing studies with the BGE_{Best} nanogel in rabbits showed positive effects. The control gel did not promote wound healing, whereas the addition of the extract accelerated the healing process. The study also demonstrated that the percentage of wound closure increased with the increase in the content of the active ingredient (BGE_{Best}). Short-term stability, skin irritation and wound-healing studies of the formulation along with positive panellist feedback, confirm the viability and acceptance of the nanogel formulation for topical use.

Future applications of the nanogel could explore its effectiveness against other severe bacterial skin infections. Additionally, other types of hydrogels can be formulated using natural polymers, such as chitosan, pectin, gelatin, and agar (alongside synthetic polymers like Carbopol® 940), to create safe nanogels suitable for both human use and environmental sustainability. There is also significant potential for utilizing the other pharmacological and biological properties of black garlic extract, such as its antioxidant, anti-inflammatory, and anti-allergic effects, for the formulation of nanogels, hydrogels, and ointments. Further investigation into the underlying mechanisms of these findings could provide valuable insights.

ACKNOWLEDGEMENTS

Authors acknowledge FIST-II, Department of Physics, Jadavpur University for FE-SEM analysis; Indian Association for the Cultivation of Science (IACS), Kolkata, India for FT-IR and ATR analyses, and Bose institute, Kolkata, India for LC-ESI-MS analysis.

CONFLICT OF INTEREST

The authors declare no competing interests.

AUTHORS' CONTRIBUTIONS

Mariah Sadaf and Anamika Das are responsible for carrying out the study, analysing the data, interpreting the findings, and writing the article. Satadal Das was responsible for designing the study and interpreting the findings of assays related to antimicrobial activity. Subhankar Saha and Ketousetuo Kuotsu were responsible for animal handling and designing the study related to skin irritation and wound-healing. Paramita Bhattacharjee was responsible for formulating the research question(s), designing the study, analysing the data, interpreting the findings, and editing the manuscript.

ORCID ID

P. Bhattacharjee https://orcid.org/0000-0002-5620-1675

REFERENCES

1. Onyeagba RA, Ugbogu OC, Okeke CU, Iroakasi O. Studies on the antimicrobial effects of garlic (*Allium sativum* Linn), ginger (*Zingiber officinale* Roscoe) and lime (*Citrus aurantifolia* Linn). Afr J Biotechnol. 2004;3:552-54. https://doi.org/10.5897/AJB2004.000-2108.
2. Singh R, Singh K. Garlic: A spice with wide medicinal actions. J Pharmacogn Phytochem. 2019;8:1349-55.
3. Shang A, Cao SY, Xu XY, Gan RY, Tang GY, Corke H, Mavumengwana V, Li HB. Bioactive compounds and biological functions of garlic (*Allium sativum* L.). Foods. 2019;8:246. https://doi.org/10.3390%2Ffoods8070246.
4. *de* Rooij BM, Boogaard PJ, Rijksen DA, Commandeur JN, Vermeulen NP. Urinary excretion of n-acetyl-s-allyl-L-cysteine upon garlic consumption by human volunteers. Arch Toxicol. 1996;70:635-39. https://doi.org/10.1007/s002040050322.

5. Dorrigiv M, Zareiyan A, Hosseinzadeh H. Garlic (*Allium sativum*) as an antidote or a protective agent against natural or chemical toxicities: A comprehensive update review. Phytother Res. 2020;34:1770-97. https://doi.org/10.1002/ptr.6645.
6. Yoo JM, Sok DE, Kim MR. Anti-allergic action of aged black garlic extract in RBL-2H3 cells and passive cutaneous anaphylaxis reaction in mice. J Med Food. 2014;17:92-102. https://doi.org/10.1089/jmf.2013.2927.
7. Amagase H, Petesch BL, Matsuura H, Kasuga S, Itakura Y. Intake of garlic and its bioactive components. J Nutr. 2001;131:955S-62S. https://doi.org/10.1093/jn/131.3.955s.
8. Bhatwalkar SB, Mondal R, Krishna SBN, Adam JK, Govender P, Anupam R. Antibacterial properties of organosulfur compounds of garlic (*Allium sativum*). Front Microbiol. 2021;12:613077. https://doi.org/10.3389/fmicb.2021.613077.
9. Lee YM, Gweon OC, Seo YJ, Im J, Kang MJ, Kim MJ, Kim JI. Antioxidant effect of garlic and aged black garlic in animal model of type 2 diabetes mellitus. Nutr Res Pract. 2009;3:156-61. https://doi.org/10.4162%2Fnrp.2009.3.2.156.
10. Jeong YY, Ryu JH, Shin JH, Kang MJ, Kang JR, Han J, Kang D. Comparison of anti-oxidant and anti-inflammatory effects between fresh and aged black garlic extracts. Molecules. 2016;21:430. https://doi.org/10.3390/molecules21040430.
11. Yuan H, Sun L, Chen M, Wang J. The comparison of the contents of sugar, Amadori, and Heyns compounds in fresh and black garlic. J Food Sci. 2016;8:C1662-68. https://doi.org/10.1111/1750-3841.13365.
12. Dunkel A, Steinhaus M, Kotthoff M, Nowak B, Krautwurst D, Schieberle P, Hofmann T. Nature's chemical signatures in human olfaction: A foodborne perspective for future biotechnology. Angew Chem Int Ed. 2014;53:7124-43. https://doi.org/10.1002/anie.201309508.
13. Mouffok A, Bellouche D, Debbous I, Anane A, Khoualdia Y, Boublia A, Benguerba Y. Synergy of garlic extract and deep eutectic solvents as promising natural Antibiotics: Experimental and COSMO-RS. J Mol Liq. 2023;375:121321. https://doi.org/10.1016/j.molliq.2023.121321.
14. Hamidi M, Azadi A, Rafiei P. Hydrogel nanoparticles in drug delivery. Adv Drug Deliv Rev. 2008;60:1638-49.

https://doi.org/10.1016/j.addr.2008.08.002.

15. Shoukat H, Pervaiz F, Khan M, Rehman S, Akram F, Abid U, Noreen S, Nadeem M, Qaiser R, Ahmad R, Farooq I. Development of β-cyclodextrin/polyvinypyrrolidone-co-poly (2-acrylamide-2-methylpropane sulphonic acid) hybrid nanogels as nano-drug delivery carriers to enhance the solubility of Rosuvastatin: An *in vitro* and *in vivo* evaluation. Plos one. 2022;17:p.e0263026. https://doi.org/10.1371/journal.pone.0263026.
16. Soni KS, Desale SS, Bronich TK. Nanogels: An overview of properties, biomedical applications and obstacles to clinical translation. J Control Release. 2016;240:109-26. https://doi.org/10.1016/j.jconrel.2015.11.009.
17. Anonymous (2020a)CN111529467A. https://r.search.yahoo.com/_ylt=AwrKD3DZKDBoQAIAh2m7HAx.;_ylu=Y29sbwNzZzMEcG9zAzEEdnRpZAMEc2VjA3Ny/RV=2/RE=1749196250/RO=10/RU=https%3a%2f%2fpatents.google.com%2fpatent%2fCN111529467A%2fen/RK=2/RS=tTpvP4nrZQ8hpUFzX9AxbGQmMmo-. Accessed 11 September 2023.
18. Safitri FI, Nawangsari D, Febrina D. Overview: Application of Carbopol 940 in Gel. In: International Conference on Health and Medical Sciences (AHMS 2020). Paris, France:Atlantis Press; 2021. pp.80-84.
19. Anonymous (2020b)Product Release Information visionCATS 3.0 (3.0.20196.1). https://r.search.yahoo.com/_ylt=AwrKBFH.YvJnCQIAF8.7HAx.;_ylu=Y29sbwNzZzMEcG9zAzEEdnRpZAMEc2VjA3Ny/RV=2/RE=1745147902/RO=10/RU=https%3a%2f%2fcamag.com%2fnews%2fproduct-release-information-visioncats-3-0-3-0-20196-1%2f/RK=2/RS=3D0bI948G9.C_RmLxUbP1HthMLY-. Accessed 07 September 2023.
20. Kanaki NS, Rajani M. Development and validation of a thin-layer chromatography-densitometric method for the quantification of alliin from garlic (*Allium sativum*) and its formulations. J AOAC Int. 2005;88:1568-70.
21. Anonymous (2023a) 13.5A: Minimal Inhibitory Concentration (MIC). https://bio.libretexts.org/Bookshelves/Microbiology/Microbiology_(Boundless)/13%3A_Antimicrobial_Drugs/13.05%3A_Measuring_Drug_Susceptibility/13.5A%3A_Minimal_Inhibitory_Concentration_(MIC)#:~:text=Minimum%20inhibitory%20concentration%20(MIC)%20can,are%20more%20effective%20antimicrobial%20agents. Accessed 28 November 2023.
22. Ghosh PK, Tamili D, Das A, Datta S, Das S, Saha S, Kuotsu K, Bhattacharjee P. Valorization of tuberose flower waste through development of therapeutic products using supercritical

carbon dioxide extraction and microencapsulation technologies. World J Microbiol Biotechnol. 2023;39:319. https://doi.org/10.1007/s11274-023-03761-7.

23. Tamili D, Jana S, Bhattacharjee P. Chromatographic method development for simultaneous determination of serotonin, melatonin, and L-tryptophan: Mass transfer modeling, chromatographic separation factors, and method prediction by artificial neural network. J Chemom. 2023;37:e3520. https://doi.org/10.1002/cem.3520.
24. Song Z, Wang Y, Li C, Tan Y, Wu J, Zhang Z. Fumigant toxicity and behavioral inhibition of garlic against red imported fire ants (*Solenopsis invicta*). Environ Sci Pollut Res. 2023;30:1889-97. https://doi.org/10.1007/s11356-022-22091-z.
25. Iizawa T, Taketa H, Maruta M, Ishido T, Gotoh T, Sakohara S. Synthesis of porous poly (*N*-isopropylacrylamide) gel beads by sedimentation polymerization and their morphology. J Appl Polym Sci. 2007;104:842-50. https://doi.org/10.1002/app.25605.
26. Zhao W, Jin X, Cong Y, Liu Y, Fu J. Degradable natural polymer hydrogels for articular cartilage tissue engineering. J Chem Technol Biotechnol. 2013;88:327-339. https://doi.org/10.1002/JCTB.3970.
27. Dyer JR. X-ray Crystallography and Mass Spectrometry of Organic Compounds. In: Applications of Absorption Spectroscopy of Organic Compounds. London: Prentice Hall, Englewood Cliffs;1965.Chapter 17,pp.143-60.
28. Buhse L, Kolinski R, Westenberger B, Wokovich A, Spencer J, Chen CW, Wolfgang E. Topical drug classification. Int J Pharm. 2005;295:101-12. https://doi.org/10.1016/j.ijpharm.2005.01.032.
29. Ghosh PK, Bhattacharjee P, Das S. Antimicrobial cream formulated with supercritical carbon dioxide extract of tuberose flowers arrests growth of *Staphylococcus aureus*. Recent Pat Biotechnol. 2016;10:86-102. https://doi.org/10.2174/1872208310666160414102732.
30. Widodo RT, Hashim H, Usir E. A comparative physicochemical and cosmetic evaluation of generic topical corticosteroid products. JUMMEC. 2002;7:114-17.
31. Damodaran S, Parkin KL, Fennema OR, editors. Food Dispersions. In: Fennema's Food Chemistry. Florida, USA: CRC press;2007; Chapter 12,pp.560.

32. Hudzicki J. Kirby-Bauer disk diffusion susceptibility test protocol. American Society for Microbiology. 2009;1-20. Accessed 12 January 2024.

33. Teshome K, Gebre-Mariam T, Asres K, Perry F, Engidawork E. Toxicity studies on dermal application of plant extract of *Plumbago zeylanica* used in Ethiopian traditional medicine. J Ethnopharmacol. 2008;117:236-48. https://doi.org/10.1016/j.jep.2008.01.036.

34. OECD (Organisation for Economic Co-operation and Development) 404 (2014) Organization of economic cooperation and development guidelines. https://r.search.yahoo.com/_ylt=AwrKCS5SE7pkO0QC0_67HAx.;_ylu=Y29sbwNzZzMEcG9zAzIEdnRpZAMEc2VjA3Ny/RV=2/RE=1689945042/RO=10/RU=https%3a%2f%2fwww.oecd-ilibrary.org%2fenvironment%2ftest-no-404-acute-dermal-irritation corrosion_9789264242678-en/RK=2/RS=zzdGFjJaMtHo4S266tnQCux5Cas-.Accessed 5 February 2024.

35. Draize JH, Woodard G, Calvery HO. Methods for the study of irritation and toxicity of substances applied topically to the skin and mucous membranes. J Pharm Exp Ther. 1944;82:377-90.

36. Lukic M, Jaksic I, Krstonosic V, Cekic N, Savic S. A combined approach in characterization of an effective w/o hand cream: The influence of emollient on textural, sensorial and *in vivo* skin performance. Int J Cosmet Sci. 2012;34:140-49. https://doi.org/10.1111/j.1468-2494.2011.00693.x.

37. Almeida IF, Gaio AR, Bahia MF. Hedonic and descriptive skin feel analysis of two oleogels: Comparison with other topical formulations. J Sens Stud. 2008;23:92-113. https://doi.org/10.1111/j.1745-459X.2007.00144.x.

38. IBM SPSS Statistics for Windows, v. 26.0. IBM Corp., Armonk, NY, USA; 2019. Available from: https://www.ibm.com/products/spss-statistics.

39. Rais N, Ved A, Ahmad R, Kumar M, Barbhai MD, Chandran D, Dey A, Dhumal S, Senapathy M, Deshmukh, VP, Anitha T. S-Allyl-L-Cysteine—A garlic Bioactive: Physicochemical nature, mechanism, pharmacokinetics, and health promoting activities. J Funct Foods. 2023;107:105657. https://doi.org/10.1016/j.jff.2023.105657.

40. Iberl B, Winkler G, Müller B, Knobloch K. Quantitative determination of allicin and alliin from garlic by HPLC. Planta Med. 1990;56:320-26. https://doi.org/10.1055/s-2006-960969.

41. Tran GB, Dam SM, Le NTT. Amelioration of single clove black garlic aqueous extract on dyslipidaemia and hepatitis in chronic carbon tetrachloride intoxicated Swiss Albino mice. Int J Hepatol. 2018;2018:9383950. https://doi.org/10.1155/2018/9383950.

42. Rahmani Z, Ghaemy M, Olad A. Preparation of nanogels based on kappa-carrageenan/chitosan and N-doped carbon dots: Study of drug delivery behavior. Polym. Bull. 2021;78:2709-26. https://doi.org/10.1007/s00289-020-03236-x.

43. Opatha SAT, Titapiwatanakun V, Boonpisutiinant K, Chutoprapat R. Preparation, characterization and permeation study of topical gel loaded with transfersomes containing asiatic acid. Molecules. 2022;27:4865. https://doi.org/10.3390/molecules27154865.

44. Wadile KA, Ige PP, Sonawane RO. Preparation of itraconazole nanoparticles and its topical nanogel: Physicochemical properties and stability studies. Int J Pharm Sci Rev Res. 2019;5:1-8. http://dx.doi.org/10.17352/ijpsdr.000020.

45. Ali A, Ali A, Rahman MA, Warsi MH, Yusuf M, Alam P. Development of nanogel loaded with lidocaine for wound-healing: Illustration of improved drug deposition and skin safety analysis. Gels. 2022;8:466. https://doi.org/10.3390/gels8080466.

46. Miastkowska M, Kulawik-Pióro A, Szczurek M. Nanoemulsion gel formulation optimization for burn wounds: Analysis of rheological and sensory properties. Processes. 2020;8:1416. https://doi.org/10.3390/pr8111416.

47. Inamdar YM, Rane B, Jain A. Preparation and evaluation of beta sitosterol nanogel: A carrier design for targeted drug delivery system. Asian J Pharm Res Dev. 2018;6:81-87. http://dx.doi.org/10.22270/ajprd.v6i3.390.

48. Agarwal S, Karar PK, Agarwal G. Semi-herbal nanogel of clindamycin phosphate and aloe vera: Formulation and evaluation. Mod appl bioequiv bioavailab. 2017;2:1-5. https://doi.org/10.19080/mabb.2017.02.555596.

49. Huang X, Brazel CS. On the importance and mechanisms of burst release in matrix-controlled drug delivery systems. J Control Release. 2001;73:121-36. https://doi.org/10.1016/S0168-3659(01)00248-6.

50. Gu B, Burgess DJ. Prediction of dexamethasone release from PLGA microspheres prepared with polymer blends using a design of experiment approach. Int J Pharm. 2015;495:393-403. https://doi.org/10.1016/j.ijpharm.2015.08.089.

51. Ahmed A, Taher M, Mandal UK, Jaffri JM, Susanti D, Mahmood S, Zakaria ZA. Pharmacological properties of Centella asiatica hydrogel in accelerating wound-healing in rabbits. BMC Complement Altern Med. 2019;19:1-7. https://doi.org/10.1186/s12906-019-2625-2.

52. Brummer R, Godersky S. Rheological studies to objectify sensations occurring when cosmetic emulsions are applied to the skin. Colloids Surf A Physicochem Eng Asp. 1999;152:89-94. https://doi.org/10.1016/S0927-7757(98)00626-8.

53. Kulawik-Pióro A, Ptaszek A, Kruk J. Effective tool for assessment of the quality of barrier creams-relationships between rheological, textural and sensory properties. Regul Toxicol Pharmacol. 2019;103:113-23. https://doi.org/10.1016/j.yrtph.2019.01.026.

54. Anonymous (2023b) What Is Argyria? https://www.webmd.com/skin-problems-and-treatments/argyria-overview. Accessed 27 September 2023.

55. Rodriguez V, Romaguera RL, Heidecker B. Silver-containing wound cream leading to Argyria-Always ask about alternative health products. Am J Med. 2017;130:e145-46. https://doi.org/10.1016/j.amjmed.2016.11.036.

56. Walker M, Cochrane CA, Bowler PG, Parsons D, Bradshaw P. Silver deposition and tissue staining associated with wound dressings containing silver. Ostomy/wound management. 2006;52:42-4.

Table 1. ESI-TOF-MS spectra of standard alliin; alliin and additional organosulfur bioactives present in BGE_{Best}

Compound	*m*/*z*	Relative absorbance/%	Source
S-allyl-L-cysteine (Alliin) [$C_6H_{11}NO_2S$] (162.22)	162.817	45	Obtained peaks in standard
S-allyl-L-cysteine (Alliin) [$C_6H_{11}NO_2S$ + H] (162.22 + 1)	163.062	100	
	163.102	95	
	163.154	85	
	163.580	80	
S-allyl-L-cysteine (Alliin) [$C_6H_{11}NO_2S$] (162.22)	162.62	90	Peaks obtained in BGE_{Best}
S-allyl-L-cysteine (Alliin) [$C_6H_{11}NO_2S$ - H] (162.22 - 1)	161.348	100	
	161.120	98	
	161.151	85	
S-allyl-L-cysteine (Alliin) [$C_6H_{11}NO_2S$ – H_2O + H + Na] (162.06 – 18 + 1 + 23)	168.211	100	
	168.243	70	
Di-allyl-disulfide (DADS) [$C_6H_{10}S_2$ + Na + H] (146.022 + 23 + 1)	170.509	100	
	170.450	70	
Di-allyl-trisulfide (DATS) [$C_6H_{10}S_3$] (177.194)	177.161	100	
	177.210	95	
	177.137	65	
Methyl-allyl-disulfide (MADS) [$C_4H_8S_2$ + H] (120.007 + 1)	121.471	100	
	121.459	85	
	120.869	80	
	121.312	70	
Methyl-allyl-trisulfide (MATS) [$C_4H_8S_3$] (151.979)	151.916	100	
	151.725	95	
	151.657	65	
	151.616	60	

Table 2. FT-IR spectrum of Carbopol® 940, DMSO, propylene glycol, lecithin soy (30 %), standard alliin, BGE_{Best}, experimental control nanogel and BGE_{Best} nanogel

Wavenumber/cm^{-1}							
Carbopol® 940	DMSO	Propylenegl ycol	Lecithin soy (30 %)	Standard alliin	BGE_{Best}	Experimental control nanogel	BGE_{Best} nanogel
3118: O-H stretching	3442: O-H stretching	3307: O-H stretching	3445: O-H stretching	3331: O-H stretching	3259: O-H stretching	3272: O-H stretching	3628,3348: O-H stretching
1713: C=O ketone stretching	2995: =C-H stretching	2969,2929, 2875: carboxylic acid OH stretching	2925: C-H stretching	2920, 2836: C-H stretching	2948: C-H stretching	2130: C-H aldehydic stretching	2853: C-H stretching
1454: CH_3 stretching	2912: C-H stretching	1455, 1411: C=C aromatic	1651,164, 1634: C-C multiple bonds stretching	1646: C=C alkene	1641, 1405: C=C alkene stretching	1635, 1420: C=C aromatic	1651: C=C alkene stretching
1114,117,12 47: C-O-C stretching	1435: C=C aromatic	1375,1331: CH_3 stretching	1732: ester stretching	1575, 1540, 1452, 1417: C=C aromatic	1118, 1013: C-O-C stretching	1077, 1039: C-O-C stretching	1249,1225: C-O-C stretching
801,648: C-Cl stretching	1040, 1017: C-F stretching 760: C-Cl stretching	1232, 1135, 1076, 1036: C-O-C stretching	1466: $C-H_2$ bending 1377: CH_2-O-P-O 1226,108: C-N	1015: C-F stretching			1044, 1016: C-F stretching

Table 3. Physicochemical analyses of the newly developed topical nanogels

Property	Experimental control nanogel	BGE_{Best} nanogel
Appearance	Clear	Pale yellow
Specific gravity	1.038	1.021
pH (25 °C)	6.90	6.82
Mass loss on drying (dry basis)/%	2.31	1.5
Spreadability/(g/(cm·s))	15.92	12.41
Centrifuge test	No phase separation	No phase separation
Phase separation at 37 °C	No phase separation	No phase separation
Phase separation at 55 °C	No phase separation	No phase separation
HLB value	17	18.6
Apparent viscosity	18.92 cP	23.03 cP
Average particle size (FE-SEM)	286.06 nm	217.77 nm

Values are reported as mean±standard deviation (S.D.)

Table 4. The wound-healing area on each day post application of positive control gel, experimental control nanogel and BGE_{Best} nanogel (2 and 4 %)

t/day	*A*/mm^2			
	R1 (positive control gel)	R2 (experimental control nanogel)	R3 (2 % BGE_{Best} nanogel)	R4 (4 % BGE_{Best} nanogel)
0	7.5	4.5	4.5	6.5
1	5	4.5	4	6
2	3	4.5	3.5	4.5
3	1		2.5	3.5
4			2	2.5
5			1.5	1.5
6			1.5	1.5

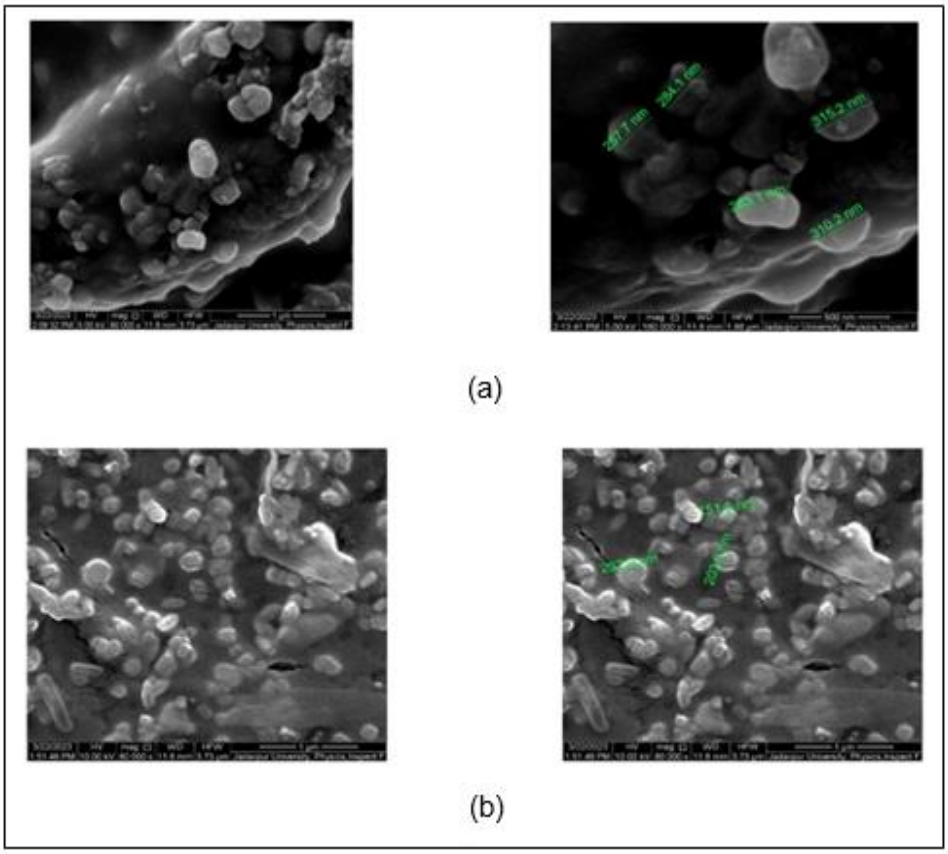

Fig. 1. FE-SEM images for: a) experimental control nanogel and b) BGE_{Best} nanogel

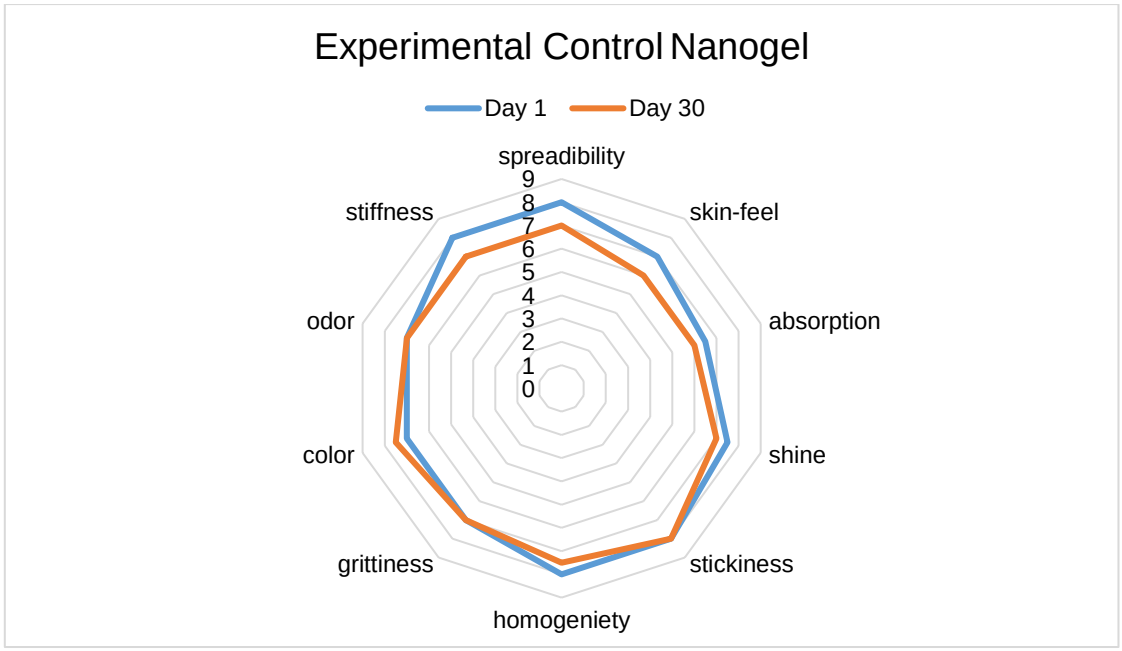

a)

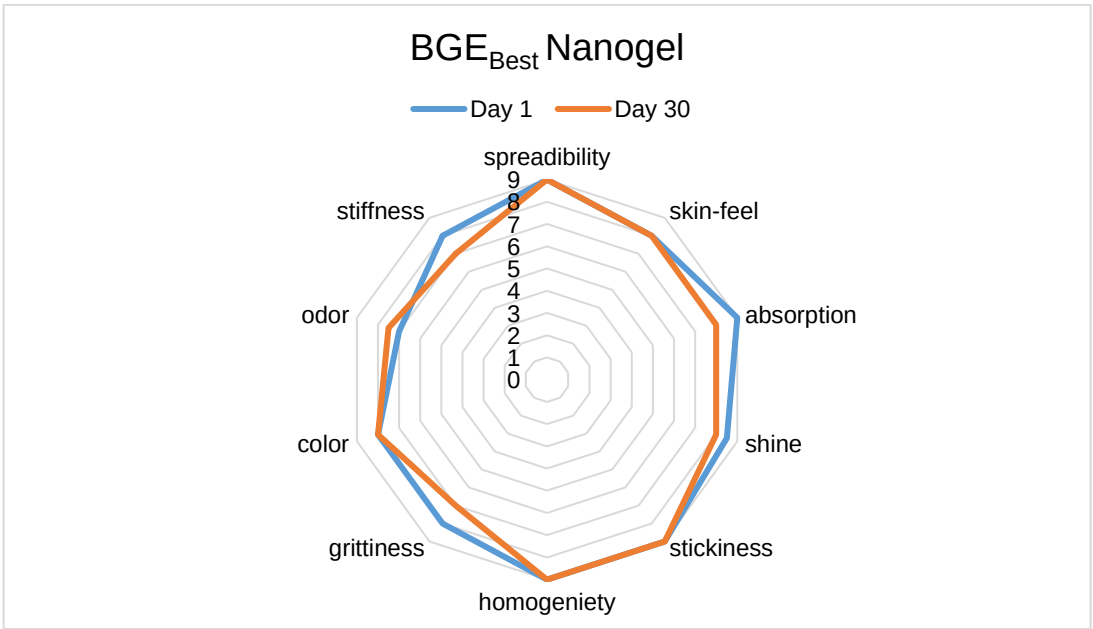

b)

Fig. 2. Radar plot of hedonic scores obtained by sensory analyses of: a) experimental control nanogel and b) BGE_{Best} nanogel on day 1 and 30

SUPPLEMENTARY MATERIAL

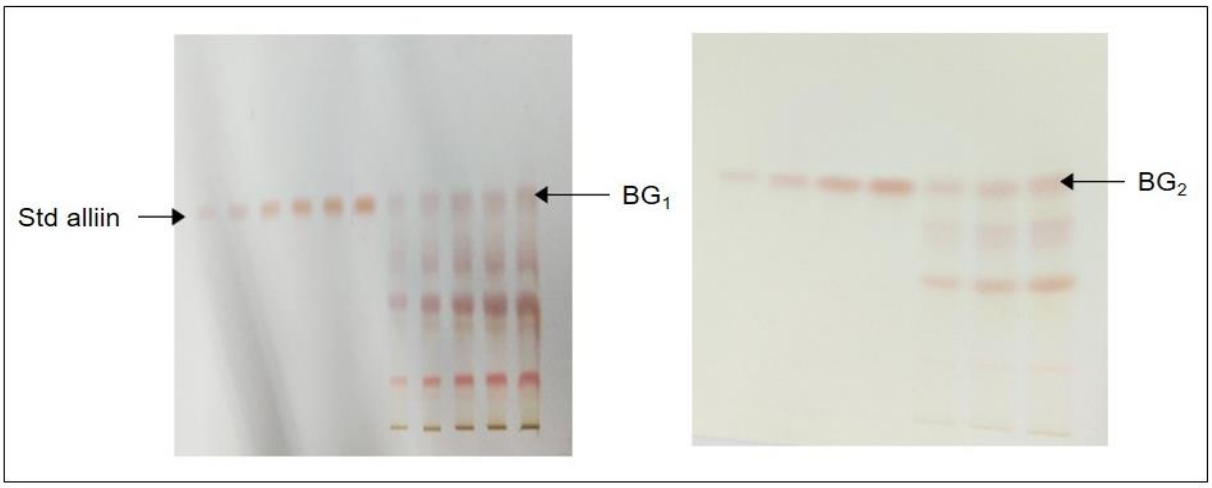

a) b)

Fig. S1. HPTLC plate for: a) BG_1 extract along with standard alliin and b) BG_2 extract

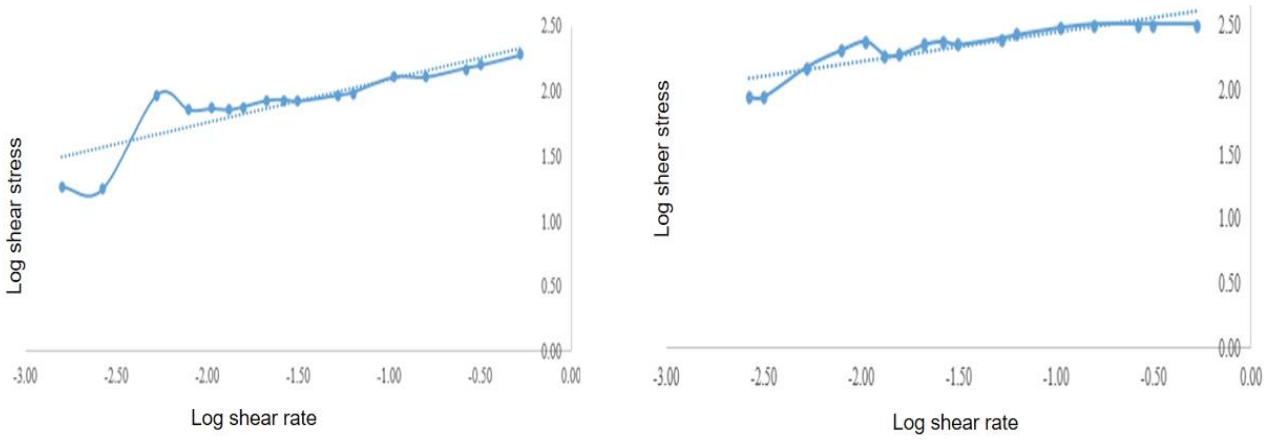

a) b)

Fig. S2. Viscosity graph for log shear stress *vs* log shear rate using modified Casson equation for: a) experimental control nanogel and b) BGE_{Best} nanogel

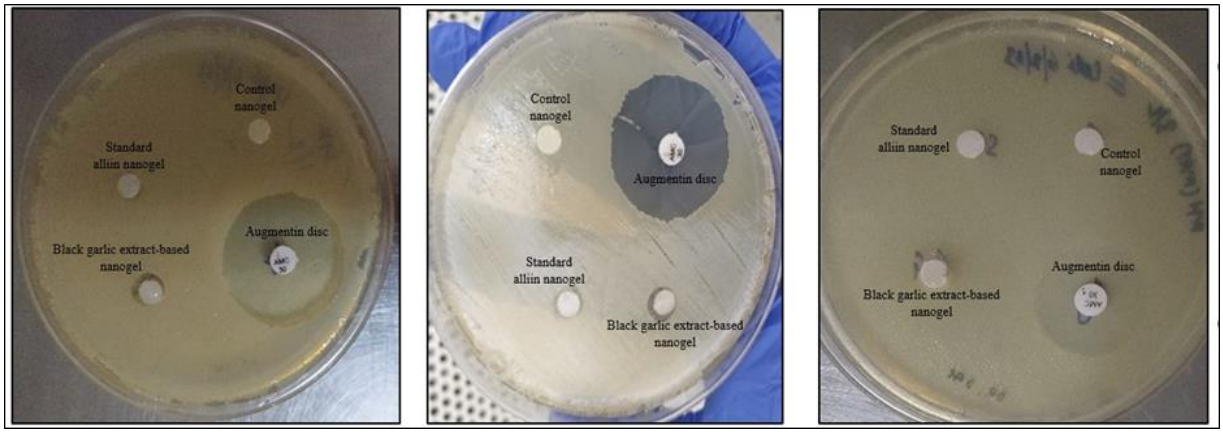

a) b) c)

Fig. S3. Zones of inhibition for standard alliin-based nanogel and BGE_{Best} nanogel against: a) *Staphylococcus aureus* (ATCC), b) *Escherichia coli* (ATCC) and c) *Escherichia coli* (MDR)

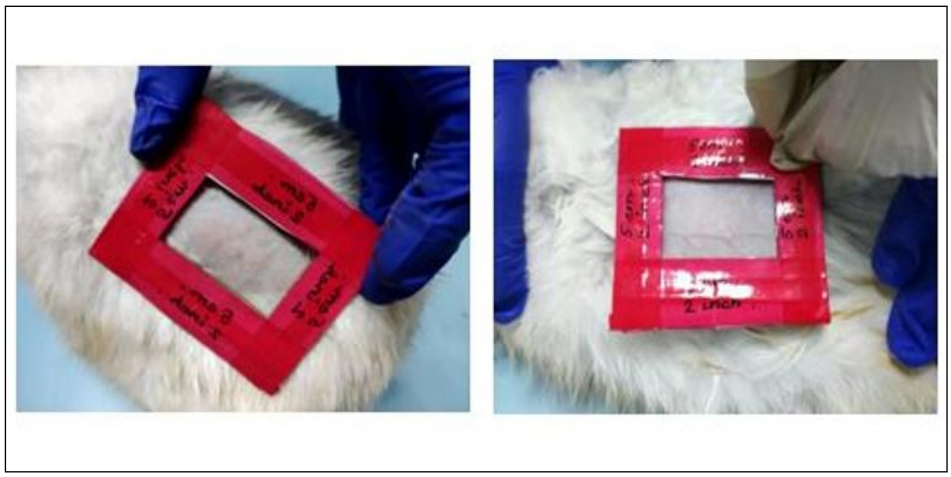

a) b)

Fig. S4. Skin irritation test of BGE_{Best} nanogel on New Zealand white rabbits: a) demarcated area on dorsal skin immediately after application (0 h) and b) post application observation after 72 h

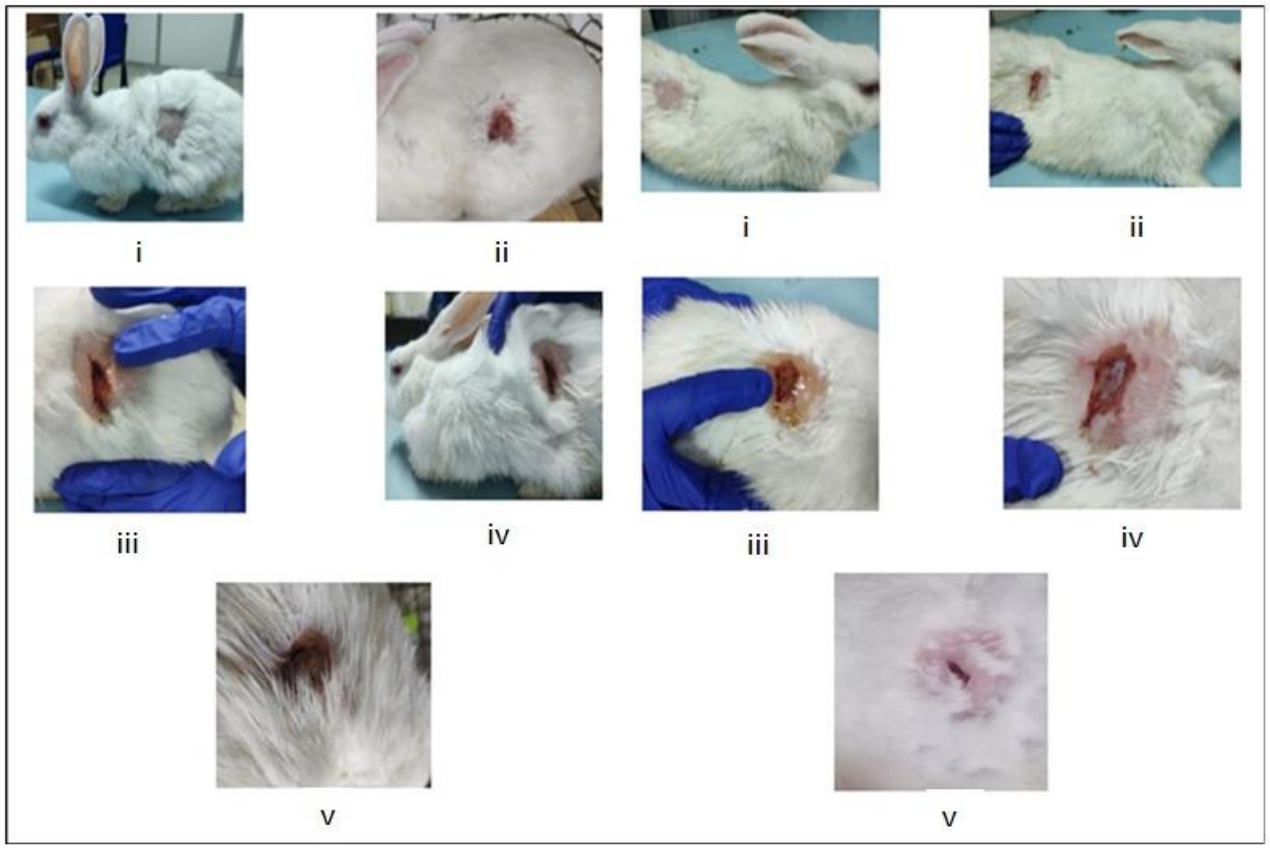

a) b)

Fig. S5. a) Wound-healing test on R3 using BGE_{Best} nanogel (2 %) i. before wound creation, ii. wound created, iii. post application observation on day 0, iv. initiation of tissue epithelization on day 3, v. wound closure on day 6. b) Wound-healing test on R4 using BGE_{Best} nanogel (4 %) i. before wound creation, ii. created wound, iii. post application observation on day 0, iv. initiation of tissue epithelization on day 2, v. wound closure on day 6